Contribution from the Laboratoire de Chimie Organique des Substances Naturelles (UA 31), Département de Chimie, Université Louis Pasteur, the Laboratoire de Chimie Physique et d'Electroanalyse (UA 405), EHICS, the Laboratoire de Chimie Minérale (UA 405), EHICS, and the Laboratoire de Cristallographie Biologique, IBMC du CNRS, Strasbourg, France

Crystallographic Study and Ligand Substitution Reactions of Dirhodium(II) Tris- and Tetrakis(tritolylbenzoate)

Henry J. Callot,*,† Anne-Marie Albrecht-Gary,‡ Malak Al Joubbeh,‡ Bernard Metz,§ and François Metz†,∥

Received February 16, 1989

The structure and coordination behavior of sterically crowded dirhodium(II) carboxylates that selectively catalyze the syn transfer of carbalkoxycarbene moieties onto *Z*-olefins are reported. Two complexes, $[Rh_2(TTB)_3(CH_3CO_2)(py)_2]$ (TTB = 2,4,6-tri-*p*-tolylbenzoate) and $[Rh_2(TTB)_4(py)_2]$, $3(py)_2$ and $4(py)_2$, respectively, have been characterized by single-crystal X-ray diffraction. The observed Rh–Rh bond distances are short: 2.401 (1) Å in $3(py)_2$ and 2.372 (2) Å in $4(py)_2$. The steric constraints induced by the carboxylic ligands around the dimetallic centers are reflected in the O–Rh–Rh–O torsion angles, whose values lie between 7 and 15°. Each metal center is at the bottom of a parallelepipedic box whose walls are built up with the *o*-tolyl groups of the benzoate ligands. In $4(py)_2$, the two pyridine ligands, which fit well inside these cavities in a diagonal orientation, are deeply buried and inaccessible. In $3(py)_2$, one side of each box is removed, permitting a lateral approach of an olefin toward a group bound to rhodium. This is also made easier by a widening of the box. The coordination of pyridine to **3**, **4**, and dirhodium(II) pivalate (**5**), used as a reference compound, shows an isosbestic behavior for both mono- and bis(pyridine) adducts. Thermodynamic data clearly indicate a large stabilization (2–3 orders of magnitude) of both adducts with the sterically hindered complexes **3** and **4** and the classical decrease of stability of the 2:1 vs the 1:1 adducts. The formation rate constants of both pyridine adducts were measured by using a stopped-flow technique. Their important slowing down with regard to the corresponding constants for **5** and the overall inertness of the adducts illustrate the peculiar geometry created by the walls in compounds **3** and **4**. In agreement with previous kinetic works, the formation rate constants of the 2:1 adducts are 10–100 times greater than the corresponding kinetic parameters for the 1:1 adducts. The lability of the second pyridine molecule bound to the dirhodium(II) carboxylates is 4–5 orders of magnitude greater than that of the first pyridine. The geometry of the carboxylate ligands gives a clue to the catalytic activity of **3** ("open" box; active) and *4* ("closed" box; inactive). An interpretation of the stereoselectivity of the carbene transfer is also proposed. Complex $3(py)_2$ crystallizes in the triclinic space group $P\bar{1}$, with a = 15.818 (2) Å, b = 20.759 (1) Å, c = 14.181 (2) Å, α = 99.85 (1)°, β = 109.80 (1)°, γ = 103.14 (1)°, and V = 4107 (2) Å^3, with Z = 2. Complex $4(py)_2$ crystallizes in the tetragonal space group $I4$, with a = 17.402 (2) Å, c = 17.643 (2) Å, and V = 5342 (2) Å^3, with Z = 2.

The catalytic cyclopropanation of olefins with diazo compounds is a highly effective reaction that has been used over almost a century.[1] In particular, the use in the recent years of soluble catalysts like rhodium(II) carboxylates[2] improved the scope of the synthesis (homogeneous conditions, low temperature, very low catalyst/substrate ratio). The reaction, which is thought to proceed via a metal–carbenoid complex has been discussed and reviewed in detail in the recent literature.[1] While most reagents show a stereochemical preference for the production of *syn*-cyclopropanes the reactions involving diazoesters give the *anti*-cyclopropylesters as major products (Scheme I).

Several attempts have been made in the past to modify the stereochemical course of the diazoester reactions but with little success.[3-5] A significant increase of the syn/anti ratio was however observed when we introduced sterically hindered rhodium(III) porphyrins as catalysts,[6] but only the use of highly modified rhodium(II) carboxylates,[7] viz. tris(triarylbenzoates) **1**

1$(L)_z$: $x = 3$; $y = 1$
2$(L)_z$: $x = 4$; $y = 0$
3$(L)_z$: Ar = Ar′ = *p*-tolyl; $x = 3$; $y = 1$
4$(L)_z$: Ar = Ar′ = *p*-tolyl; $x = 4$; $y = 0$

($(L)_2 = (H_2O)_2$), produced selectively *syn*-cyclopropanes (syn/anti ratio in the 2–4 range for cyclohexene, depending on the structure of the catalyst). Space-filling models suggested that the *o*-aryl groups build a rigid wall around the catalytic site, leaving only a rather narrow entrance for the olefin at the site occupied by the remaining acetate. The absence of catalytic activity for **2** ($(L)_2 = (H_2O)_2$), in which the fourth ligand was supposed to block any access for the substrate, was in favor of this interpretation.

Scheme I

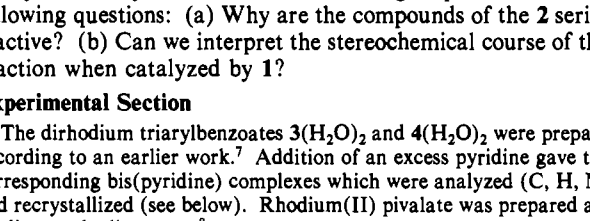

In this article, we will describe the catalytic sites of these highly hindered rhodium carboxylates by using two approaches: (a) the structural determination by X-ray diffraction of the bis(pyridine) complexes $3(py)_2$ and $4(py)_2$; (b) a thermodynamical and kinetical analysis of the complexation of pyridine on both rhodium sites of **3** and **4**. These results will then be utilized for discussing the catalytic activity of **1** and **2** and answering, if possible, the two following questions: (a) Why are the compounds of the **2** series inactive? (b) Can we interpret the stereochemical course of the reaction when catalyzed by **1**?

Experimental Section

The dirhodium triarylbenzoates $3(H_2O)_2$ and $4(H_2O)_2$ were prepard according to an earlier work.[7] Addition of an excess pyridine gave the corresponding bis(pyridine) complexes which were analyzed (C, H, N) and recrystallized (see below). Rhodium(II) pivalate was prepared according to the literature.[8]

† UA 31.
‡ UA 405.
§ UA 405 and IBMC.
∥ Present address: Centre de Recherches des Carrières, Rhône-Poulenc, 69192 St Fons, France.

(1) Doyle, M. P. *Chem. Rev.* **1986**, *86*, 919; *Acc. Chem. Res.* **1986**, *19*, 348 and references cited therein.
(2) Hubert, A. J.; Noels, A. F.; Anciaux, A. J.; Teyssié, P. *Synthesis* **1976**, 600. Anciaux, A. J.; Hubert, A. J.; Noels, A. F.; Petiniot, N.; Teyssié, P. *J. Org. Chem.* **1980**, *45*, 695. Anciaux, A. J.; Demonceau, A.; Noels, A. F.; Hubert, A. J.; Warin, R.; Teyssié, P. *J. Org. Chem.* **1981**, *46*, 873. Anciaux, A. J.; Demonceau, A.; Noels, A. F.; Warin, R.; Hubert, A. J.; Teyssié, P. *Tetrahedron* **1983**, *39*, 2169.
(3) Moser, W. R. *J. Am. Chem. Soc.* **1969**, *91*, 1135.
(4) Holland, D.; Milner, D. J. *J. Chem. Res., Synop.* **1979**, 317.
(5) Doyle, M. P.; Dorrow, R. L.; Buhro, W. E.; Griffin, J. H.; Tamblyn, W. H.; Trudell, M. L. *Organometallics* **1984**, *3*, 44 and references cited therein.
(6) Callot, H. J.; Metz, F.; Piechocki, C. *Tetrahedron* **1982**, *38*, 2365.
(7) Callot, H. J.; Metz, F. *Tetrahedron* **1985**, *41*, 4495.
(8) Legzdins, P.; Mitchell, R. W.; Rempel, G. L.; Ruddick, J. D.; Wilkinson, G. *J. Chem. Soc. A* **1970**, 3322.

0020-1669/89/1328-3633$01.50/0

Table I. Crystallographic Data

	$3(py)_2$	$4(py)_2$
space group	$P\bar{1}$	$I4$
cell const		
a, Å	15.818 (2)	17.402 (2)
b, Å	20.759 (1)	
c, Å	14.181 (2)	17.643 (2)
α, deg	99.85 (1)	
β, deg	109.80 (1)	
γ, deg	103.14 (1)	
V, Å^3	4107 (2)	5342 (2)
Z, formula units/cell	2	2
formula	$C_{96}H_{82}N_2O_8Rh_2$	$C_{122}H_{102}N_2O_8Rh_2$
fw[a]	1597.57	1929.99
d_{calcd}, g cm^{-3}	1.29	1.20
d_{obsd},[b] g cm^{-3}	1.30 (1)	1.23 (1)
μ(Cu Kα), cm^{-1}	37.56	29.61
radiation, Å	1.541 84	1.541 84
cryst dimens, mm	0.08 × 0.11 × 0.20	0.16 × 0.20 × 0.24
max, min, av transm factors	1.00, 0.696, 0.862	1.00, 0.93, 0.96
color	dark purple	dark purple
scan type	$\omega/2\theta$	$\omega/2\theta$
scan width, deg	0.7 + 0.14 tan θ	0.6 + 0.14 tan θ
data collection range (θ), deg	2–56	2–72
no. of unique data	10664	2727
no. of data, $I > 3\sigma(I)$	5432	2179
p	0.06	0.08
no. of refined variables	977	300
$R = \sum\|\|F_o\| - \|F_c\|\|/\sum\|F_o\|$	0.059	0.070
$R_w = [\sum w(\|F_o\| - \|F_c\|)^2/\sum w\|F_o\|^2]^{1/2}$	0.071	0.101
GOF = $[\sum w(\|F_o\| - \|F_c\|)^2/(NO - NV)]^{1/2}$	1.34	1.65
largest peak (final diff Fourier map), e Å^{-3}	0.70	1.28
largest shift/esd (final least-squares cycle)	0.47	0.01

[a] For the given formula (without the solvent). [b] Flotation in an aqueous potassium tartrate solution.

X-ray Crystallographic Procedures. Crystals of the complex $3(py)_2$ were obtained by allowing methanol to slowly diffuse into a chlorobenzene solution and those of complex $4(py)_2$ by a slow cooling of a chlorobenzene/acetone solution. Crystals suitable for X-ray diffraction studies were sealed in Lindemann glass capillaries. The diffraction data of both $3(py)_2$ and $4(py)_2$ were collected at 20 ● 1 °C on an Enraf-Nonius CAD4 diffractometer using graphite-monochromated Cu Kα radiation.[9]

The crystal parameters and other interesting data are summarized in Table I. Intensity data for $3(py)_2$ and $4(py)_2$, gathered by the ω–2θ scan technique, were reduced by routine procedures. The intensities of three standard reflections were measured every 2 h of X-ray exposure time, and no decay was observed. The net intensities and their standard deviations were corrected for Lorentz and polarization effects. An empirical absorption correction was applied by use of ψ scans of several reflections with diffractometer angle χ near 90° for both $3(py)_2$ and $4(py)_2$. Reflections having $I > 3\sigma(I)$ were included in the refinement. The weight of each reflection was calculated as $w = 4F_o^2/\sigma^2(F_o^2)$, with $\sigma(F_o^2) = [\sigma(I)^2 + (pF_o^2)^2]^{1/2}$ and $\sigma(I)$ based on counting statistics. The atomic scattering factors were taken from the usual tabulation,[10] and the effects of anomalous dispersion were included in F_c.[11] All calculations were done by using SDP.[9] Relevant details for both structure determinations are given below.

Compound $3(py)_2$. The automatic locating and centering of 23 reflections ($20 < \theta < 30°$) followed by least-squares analyses of the setting angles produced accurate unit cell parameters, indicating the triclinic crystal system. Solution and refinement were undertaken in the space group $P\bar{1}$. The positions of the two Rh atoms were obtained from a three-dimensional Patterson map. The remaining non-hydrogen atoms were found with subsequent difference Fourier maps and least-squares refinement. The hydrogen atoms, except those of the methyl groups, were introduced at this stage after they were located on a difference Fourier map. They were introduced at the best theoretical positions (C–H = 0.95 Å, B = 6.0 Å^2). With the hydrogen atoms held fixed, the refinement was continued, including anisotropic temperature factors for the non-hydrogen atoms. A small amount (1.25 e Å^{-3}) of residual electron density was found. This appeared to be a remnant of a solvent molecule of crystallization. It was refined as an oxygen of a lattice water molecule with a fixed multiplicity of 0.37. This value had been established in an earlier refinement in which the multiplicity of the oxygen had been refined.

Compound $4(py)_2$. Final orientation matrix and cell parameters were obtained from a least-squares fit of 25 machine-centered reflections ($25 < \theta < 28°$). The cell dimensions indicated a tetragonal crystal class. The Laue class was determined to be $4/m$. The noted systematic absences and the value of Z (two dimetallic units per cell) limited the possible space groups to either $I4$, $I\bar{4}$, or $I4/m$. Since the absence of torsional twist in the tritolylbenzoate ligand seemed highly improbable (it would imply $4/m$ symmetry), space group $I4/m$ was eliminated. If space group $I4$ is chosen, the crystallographically imposed site symmetry is ($\bar{4}$). But, in this hypothesis, overlap of the symmetry-related tolyl groups is found. This can be easily seen with a molecular model. Therefore, a structural model for $4(py)_2$ was developed in the noncentrosymmetric $I4$ space group.

The position of the second rhodium atom was derived from the Patterson map. All remaining non-hydrogen atoms were identified in subsequent difference Fourier calculations. The atoms of the **4** group refined quite steadily, while the peaks assigned to the pyridine atoms did not behave well upon refinement. The pyridines were badly disordered, which prevented satisfactory completion of the structural analysis. Their nitrogen and para carbon atoms were placed on the 4-fold axis. The ortho and meta carbon atom positions were modeled in terms of disorder over 4 positions. During the refinement stage one pyridine was unexceptional, while the second showed a great thermal agitation, resulting in poor resolution.

The hydrogen atoms, except those of the pyridines, located on a difference Fourier map, were introduced in idealized positions (C–H = 0.95 Å; B = 6.0 Å^2). They were not refined. All non-hydrogen atoms except those of the pyridines were refined anisotropically. Small amounts of residual electron density were found. They correspond to solvent molecules with statistical occupancy and were not introduced. The R value for the refined inverted image and the Hamilton significance test[12] established the configuration as that originally refined, to a significance level of better than 0.005.

Coordination of Pyridine to 3, 4, and 5: Spectrophotometric, Thermodynamic, and Kinetic Studies. As starting materials, to avoid the use of strictly anhydrous conditions, we used both $3(H_2O)_2$ and $4(H_2O)_2$ as obtained from a recrystallization and storage in a "normal" humid atmosphere. Previous studies[7] confirmed the presence of one water molecule coordinate per rhodium site. As in the catalytic[7] studies, we selected $Rh_2(pivalate)_4(H_2O)_2$ ($5(H_2O)_2$) as a reference carboxylate, its solubility being high in most organic solvents. Dichloroethane (DCE; Merck, Uvasol) was chosen throughout the experiments since not only is it a good solvent for the dirhodium carboxylates but also its limited volatility was compatible with stopped-flow experiments (high volatility precluded the use of dichloromethane). To estimate the contribution of the coordinated water molecules to the data, a parallel set of measurements were run in 20% (by volume) tetrahydrofuran (THF; Merck, Uvasol) in DCE, the large molar excess of THF insuring the presence, in solution, of $3(THF)_2$, $4(THF)_2$, and $5(THF)_2$.

Spectrophotometric titrations with pyridine (Merck, Uvasol) of $3(H_2O)_2$, $4(H_2O)_2$, and $5(H_2O)_2$ in pure DCE and of their $(THF)_2$ homologues in DCE–THF (80:20 by volume) were followed in the visible region (400–800 nm). The corresponding absorption spectra were recorded by using a Cary 17D spectrophotometer and Helma quartz cuvettes (1 cm). The samples (2.5 mL) were prepared before each run at a fixed dirhodium carboxylate concentration (10^{-3} mol L^{-1}) and variable pyridine concentrations (from 10^{-4} to 8 × 10^{-3} mol L^{-1}). Typical titration curves are presented in Figure 1.

The numerical spectrophotometric data were recorded on a Periferic Zip 30 printer coupled with a digital interface to the spectrophotometer and processed with the LETAGROP-SPEFO program.[13] The stability constants and the molar absorptivities of each species formed during the titration were simultaneously refined with the program, which minimized the sum of the squares of the differences between experimental and

(9) All crystallographic work was done at the Laboratoire de Cristallographie Biologique, IBMC du CNRS, Strasbourg, France. The calculations were carried out on PDP8/A and 11/44 computers with the Enraf-Nonius CAD4-SDP-PLUS programs. This crystallographic computing package is described by: Frenz, B. A. In *Computing in Crystallography*; Schenk, H., Olthof-Hazekamp, R., van Konigsveld, H., Bassi, G. C., Eds.; Delft University Press: Delft, Holland, 1978; pp 64–71. Frenz, B. A. *Structure Determination Package and SDP-PLUS User's Guide*; B. A. Frenz, Assoc., Inc.: College Station, TX, 1982.

(10) Cromer, D. T.; Waber, J. T. *International Tables for X-Ray Crystallography*; Kynoch: Birmingham, England, 1974; Vol. IV, Table 2.2B.

(11) Cromer, D. T.; Ibers, J. A. *International Tables for X-Ray Crystallography*; Kynoch: Birmingham, England, 1974; Vol. IV, Table 2.3.1.

(12) Hamilton, W. C. *Acta Crystallogr.* **1965**, *18*, 502.

(13) Sillen, L. G.; Warnquist, B. *Ark. Kemi* **1968**, *31*, 315, 377.

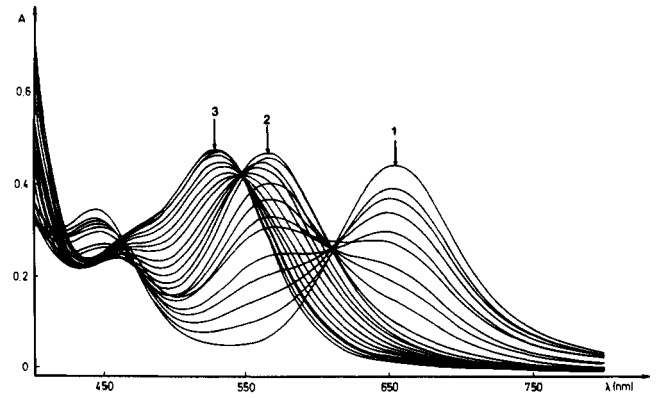

Figure 1. Evolution of the absorption spectra of $3(H_2O)_2$ with increasing pyridine concentration. Conditions: solvent, DCE; $T = 25.0 \pm 0.1°$; $[3(H_2O)_2] = 1.9 \times 10^{-3}$ mol L^{-1}. For spectra 1–3: [pyridine] = 0, 1.9×10^{-3}, and 5.7×10^{-3} mol L^{-1}, respectively. Spectra for $4(H_2O)_2$ and $5(H_2O)_2$ in DCE and spectra obtained in DCE–THF (80:20) are available as supplementary material.[15]

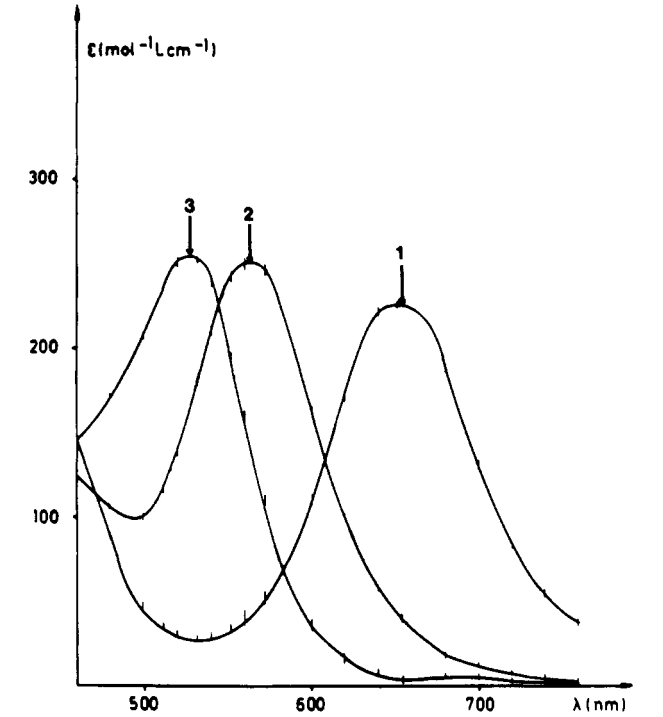

Figure 2. Calculated electronic spectra of the species formed on addition of pyridine to $3(H_2O)_2$ in DCE. Spectrum 1 is of $3(H_2O)_2$; spectra 2 and 3 correspond respectively to the 1:1 and 2:1 pyridine adducts. Spectra for $4(H_2O)_2$ and $5(H_2O)_2$ in DCE and spectra obtained in DCE–THF (80:20) are available as supplementary material.[15]

calculated absorbances at various wavelengths (the resulting curves will be referred to as "calculated spectra" in the discussion). Two species, respectively formed with one pyridine molecule and with two pyridine molecules, were identified in both solvents. Their stability constants are presented in Table IX. The calculated electronic spectra of the two species obtained during the titration of **3** with pyridine in both solvent systems are presented in Figure 2, while the values of the absorption maxima of all the species observed during the titrations are gathered in Table VIII.

The kinetic measurements were run on a Durrum-Gibson stopped-flow spectrophotometer. The data were treated on line with an Apple II microcomputer through a Datalab transient recorder DL 905 using first-order kinetics programs.[14]

The coordination of the first pyridine molecule was studied at the λ_{max} of the species formed (560–572 nm depending on the starting material and the solvent; see Table VIII). Stoichiometric conditions were realized by mixing solutions of equal concentrations (10^{-4} mol L^{-1}) of both dirhodium carboxylates and pyridine.

(14) Lagrange, P.; Lagrange, J. *J. Chim. Phys.* **1984**, *81*, 425.

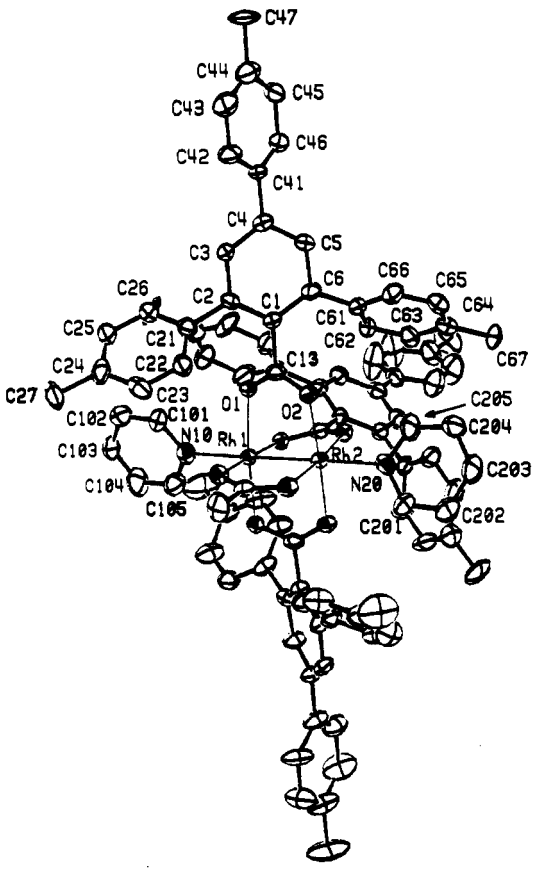

Figure 3. ORTEP view of compound $3(py)_2$, showing the atom-numbering scheme of the rhodium atoms, the pyridines, and one of the tritolylbenzoate ligands. The two remaining tritolylbenzoate ligands (with labels omitted for clarity) are numbered in an identical manner. The atoms of the acetate group are labeled OAc1, OAc2, C1, and C2. Thermal ellipsoids are at the 30% probability level. Hydrogen atoms are omitted.

To study the coordination of the second pyridine molecule, an excess of pyridine was added in the stopped-flow spectrometer to a solution containing the monopyridine adduct. The latter complex was prepared at a concentration of ca 10^{-4} mol L^{-1} and the pyridine concentrations were at least 8×10^{-4} mol L^{-1}. The wavelengths of 510 nm (**3**) and 520 nm (**4** and **5**) were selected to provide large absorption amplitudes.

Results and Discussion

Crystal Structures. Final atomic positional parameters for all non-hydrogen atoms of compounds $3(py)_2$ and $4(py)_2$ are listed in Table II. Table IIIS records their anisotropic thermal parameters.[15] Full distances and bond angles are listed in Table IVS and selected distances and angles in Table V. Least-squares planes calculations for $3(py)_2$ and $4(py)_2$ appear in Table VIS.[15]

Compound $3(py)_2$. Figures 3 and 4 display the discrete bulky dimetallic species. The coordination geometry of the metal–metal group (Rh–Rh = 2.401 (1) Å) only approximates C_4 symmetry (D_{4h} is found in all as yet studied singly bonded dirhodium tetracarboxylates[16,17]). The steric demand of the *o*-tolyl groups and their interaction with the pyridine ligands (see below) induce this loss of symmetry. It is clearly reflected in the values of the O–Rh–Rh–O torsion angles: 7.2 (3) (acetate) and 10.1 (3)° (average for the benzoates). This skewing around the Rh–Rh bond has been observed in compounds with bridging ligands comparable to the carboxylates, but possessing mixed donor atoms.[18,19]

In trans positions to the Rh–Rh bond, the pyridine nitrogen atoms are at equivalent distances (2.18 (2) and 2.20 (2) Å from

(15) See paragraph at end of paper regarding supplementary material.
(16) Agaskar, P. A.; Cotton, F. A.; Falvello, L. R.; Han, S. J. *J. Am. Chem. Soc.* **1986**, *108*, 1214 and references therein.
(17) Felthouse, T. R.; Dong, T.-Y.; Hendrickson, D. N.; Shieh, H.-S.; Thompson, M. R. *J. Am. Chem. Soc.* **1986**, *108*, 8201.
(18) Lifsey, R. S.; Lin, X. Q.; Chavan, M. Y.; Ahsan, M. Q.; Kadish, K. M.; Bear, J. L. *Inorg. Chem.* **1987**, *26*, 830.
(19) Cotton, F. A.; Felthouse, T. R. *Inorg. Chem.* **1981**, *20*, 584.

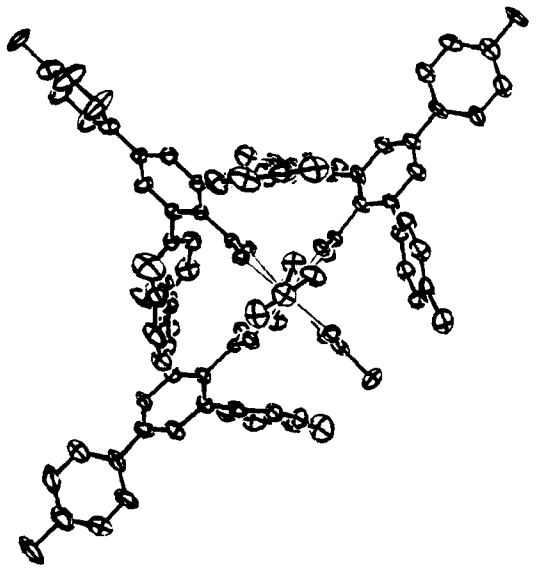

Figure 4. Top view of compound $3(py)_2$.

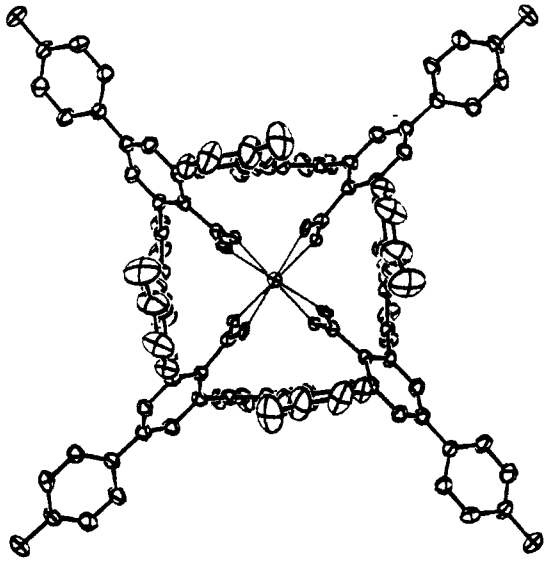

Figure 5. Top view of compound $4(py)_2$ (pyridines omitted).

each Rh). These distances are in agreement with those measured for various nitrogen-bonded adducts of $Rh_2(O_2CR)_4$.[20,21] The axial pyridine nitrogen atoms are nearly colinear with the Rh–Rh bond (Rh1–Rh2–N2O = 179.0 (2)°; Rh2–Rh1–N10 = 178.7 (3)°). Each Rh atom is displaced about 0.09 Å out of the equatorial plane of four carboxylate oxygen atoms toward the nitrogen atom. The average Rh–O bond distance is 2.041 (9) Å. Bond distances and angles are collected in Table IVS. In the tritolylbenzoate groups the *o*-tolyl moieties are slightly forced out from the 4-fold axis (average value for C1–C2–C21 and C1–C6–C61 angles of 125°). The same effect is observed in $4(py)_2$.

Compound $4(py)_2$. An ORTEP view of **4** is shown in Figure 5. The numbering scheme is similar to that used in $3(py)_2$. The Rh–Rh bond length of 2.374 (3) Å is at the short end of the range for $Rh_2(O_2CR)_4$ complexes.[20,22,23] The average Rh–O bond distance is 2.050 (8) Å, similar to that found in $3(py)_2$. The displacement of each Rh toward the nitrogens out of the equatorial plane of four carboxylate oxygen atoms is dissymmetric: 0.17 Å for Rh2 and only 0.02 Å for Rh1. The Rh–N bond lengths are Rh1–N10 = 2.28 (4) Å and Rh2–N20 = 2.21 (3) Å.

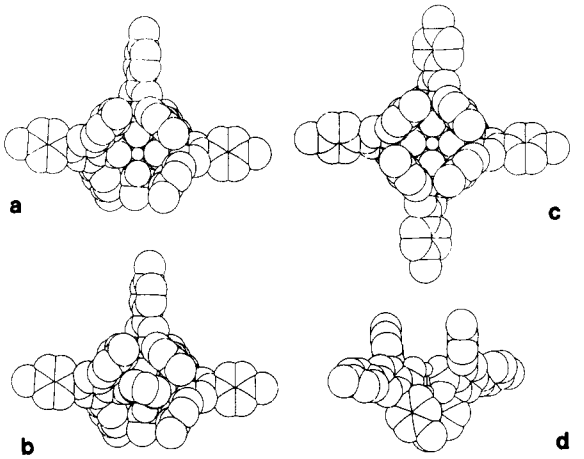

Figure 6. PLUTO space-filling drawings. Assumed van der Waals or ionic radii are as follows (Å): C, 1.70; N, 1.50; O, 1.40; Rh^{2+}, 0.70. Hydrogen atoms are omitted. Key: (a) $3(py)_2$ (pyridines omitted); (b) $3(py)_2$; (c) $4(py)_2$ (pyridines omitted); (d) sideview of $4(py)_2$, with two "trans" tritolylbenzoate ligands omitted in order to show the trench in which the axial ligands are placed.

The equatorial positions of $4(py)_2$ are staggered, the twist angle around the Rh–Rh bond being equal to 14.7 (3)°; the greatest as yet observed value for a O–Rh–Rh–O torsion angle.[19] This twist is due to the repulsive forces between the bulky tritolylbenzoate groups, the effect being obviously larger than in $3(py)_2$. It keeps away from each other the adjacent "axial" tolyl groups (in the ortho position with respect to the carboxylate) of vicinal ligands. The shortest observed H···H contact is equal to 2.33 Å to compare with the van der Waals radius value for hydrogen in the range 1.20–1.45 Å.[24] Two small values (18.0 and 29.6°) are observed for the dihedral angles between the planar aromatic rings (Table VIII). This also can only be interpreted in terms of steric crowding.

Cavities in 3 and 4. The unit **4** possesses a 4-fold axis that passes through the rhodium atoms; the $Rh_2(O_2C)_4$ core has D_4 point symmetry. The mean planes of the axial *o*-tolyl groups are roughly parallel to the Rh–Rh axis and the groups are placed in a perpendicular geometry with regard to each other. They determine on both sides of structure **4** two tetragonal prismatic "boxes". The two pyridines, not represented in Figure 5, enter in these boxes to bind the Rh atoms. One wall of each box is absent in **3**, thus leaving, on two perpendicular faces, an open "window".

In Figure 6 the van der Waals radii of the C, N, O, and Rh atoms are taken into account to give a better representation of the boxes, windows, and ligands. Parts a (**3**), b ($3(py)_2$), and c (**4**) of Figure 6 are viewed along the Rh–Rh axis while Figure 6d gives a sideview of the trench between opposite walls in **4**.

The dimensional parameters of these boxes—height and width at various distances from the O_4 planes—have been evaluated from the structural data. In $4(py)_2$ the width at the bottom of the boxes, the O_4 plane, is derived from the length of the diagonal that joins the centers of two nonadjacent central phenyl rings times $1/\sqrt{2}$. The obtained value is 7.8 Å. An approximate width at different heights is derived from the distance between pairs of carbon atoms related by a rotation of π about the z axis. One pair of each ortho, meta, and para carbon of the parallel axial tolyl groups meets approximately these requirements. The range of the corresponding distances for the two boxes in $4(py)_2$ is 8.0–8.3 Å. Subtracting the thickness of the π-system leaves an effective width available for the pyridine of 4.4–4.9 Å perpendicular to the walls or 6.2–6.9 Å along the diagonal. In the case of **3**, the replacement of one tritolylbenzoate ligand by a small acetate group induces some additional deformation, but the image is still valid. The corresponding values range from 4.5 to 6.0 Å perpendicular to the walls

(20) Cotton, F. A.; Thompson, J. L. *Inorg. Chim. Acta* **1984**, *81*, 193.
(21) Koh, Y. B.; Christoph, G. G. *Inorg. Chem.* **1978**, *17*, 2590.
(22) Cotton, F. A.; Walton, R. A. *Multiple Bonds Between Metal Atoms*; Wiley: New York, 1982.
(23) Felthouse, T. R. *Prog. Inorg. Chem.* **1982**, *29*, 73.
(24) Bondi, A. *J. Phys. Chem.* **1964**, *68*, 441–451. Allinger, N. L.; Hirsch, J. A.; Miller, M. A.; Tyminski, I. J.; Van-Catledge, F. A. *J. Am. Chem. Soc.* **1968**, *90*, 1199. Gavezzotti, A. *J. Am. Chem. Soc.* **1984**, *105*, 5220.

Table II. Positional Parameters and Their Estimated Standard Deviations

atom	x	y	x	B_{eq},[a] Å^2	atom	x	y	x	B_{eq},[a] Å^2
				(1) **3**$(py)_2$					
Rh1	0.82554 (5)	0.33047 (4)	0.23449 (7)	3.45 (2)	C5b	0.7943 (8)	0.0368 (5)	0.3571 (9)	4.7 (3)
Rh2	0.84662 (5)	0.25082 (4)	0.10673 (7)	3.56 (2)	C6b	0.8144 (7)	0.0877 (5)	0.3081 (8)	3.9 (3)
OAc1	0.8498 (5)	0.4028 (4)	0.1584 (6)	5.0 (2)	C21b	0.6520 (7)	0.1895 (6)	0.3520 (9)	5.1 (4)
OAc2	0.8872 (5)	0.3311 (4)	0.0498 (5)	4.4 (2)	C22b	0.5938 (8)	0.1988 (7)	0.265 (1)	6.9 (4)
C1	0.8786 (7)	0.3888 (6)	0.0866 (9)	5.0 (4)	C23b	0.5454 (8)	0.2469 (6)	0.270 (1)	7.7 (4)
C2	0.9050 (9)	0.4484 (6)	0.036 (1)	6.5 (4)	C24b	0.5515 (8)	0.2870 (7)	0.360 (1)	7.6 (5)
N10	0.8050 (6)	0.4016 (5)	0.3532 (7)	5.3 (3)	C25b	0.6082 (9)	0.2763 (8)	0.447 (1)	9.4 (5)
C101	0.7285 (8)	0.4201 (6)	0.333 (1)	6.0 (4)	C26b	0.6578 (8)	0.2284 (7)	0.447 (1)	7.5 (5)
C102	0.7106 (9)	0.4613 (7)	0.405 (1)	7.1 (5)	C27b	0.4960 (9)	0.3371 (7)	0.360 (1)	10.7 (6)
C103	0.7775 (9)	0.4871 (6)	0.505 (1)	6.4 (4)	C41b	0.7051 (8)	−0.0206 (6)	0.4528 (9)	5.2 (4)
C104	0.858 (1)	0.4702 (7)	0.530 (1)	8.1 (5)	C42b	0.663 (1)	−0.0159 (7)	0.521 (1)	11.0 (5)
C105	0.8692 (9)	0.4278 (7)	0.450 (1)	6.4 (4)	C43b	0.643 (1)	−0.0707 (8)	0.565 (1)	11.0 (5)
N20	0.8686 (6)	0.1797 (5)	−0.0079 (7)	5.3 (3)	C44b	0.660 (1)	−0.1305 (7)	0.544 (1)	7.9 (5)
C201	0.9517 (8)	0.1861 (7)	−0.013 (1)	6.7 (4)	C45b	0.704 (1)	−0.1334 (7)	0.481 (1)	9.7 (6)
C202	0.9707 (9)	0.1431 (8)	−0.084 (1)	8.2 (5)	C46b	0.729 (1)	−0.0785 (7)	0.436 (1)	7.9 (5)
C203	0.8959 (9)	0.0884 (7)	−0.156 (1)	7.7 (5)	C47b	0.636 (1)	−0.1875 (7)	0.595 (1)	9.5 (5)
C204	0.8079 (9)	0.0798 (7)	−0.154 (1)	8.3 (5)	C61b	0.8914 (7)	0.0873 (5)	0.2698 (8)	4.2 (3)
C205	0.7999 (9)	0.1278 (7)	−0.077 (1)	6.5 (4)	C62b	0.9852 (8)	0.1128 (8)	0.339 (1)	7.8 (5)
O1a	0.9672 (4)	0.3585 (3)	0.3192 (5)	4.3 (2)	C63b	1.0575 (9)	0.1139 (9)	0.305 (1)	9.6 (6)
O2a	0.9815 (4)	0.2705 (4)	0.2134 (6)	4.5 (2)	C64b	1.0442 (9)	0.0906 (7)	0.204 (1)	7.3 (5)
C11	1.0117 (7)	0.3191 (5)	0.2946 (8)	4.1 (3)	C65b	0.9525 (8)	0.0623 (7)	0.138 (1)	6.7 (4)
C1a	1.1151 (7)	0.3343 (5)	0.3696 (8)	4.0 (3)	C66b	0.8753 (8)	0.0615 (6)	0.1672 (9)	5.3 (4)
C2a	1.1390 (7)	0.3426 (6)	0.4771 (8)	4.3 (3)	C67b	1.1231 (8)	0.0905 (8)	0.163 (1)	9.7 (5)
C3a	1.2333 (7)	0.3549 (6)	0.5407 (9)	4.9 (4)	O1c	0.6847 (4)	0.2938 (3)	0.1396 (5)	3.9 (2)
C4a	1.3035 (7)	0.3620 (6)	0.5062 (9)	5.1 (4)	O2c	0.7097 (4)	0.2333 (3)	0.0105 (5)	4.2 (2)
C5a	1.2790 (7)	0.3550 (6)	0.4009 (9)	5.0 (4)	C13	0.6572 (7)	0.2559 (5)	0.0514 (8)	4.2 (3)
C6a	1.1860 (7)	0.3410 (6)	0.3283 (8)	4.2 (3)	C1c	0.5525 (7)	0.2329 (5)	−0.0156 (8)	4.0 (3)
C21a	1.0712 (7)	0.3416 (6)	0.5293 (9)	5.3 (4)	C2c	0.5033 (7)	0.2810 (5)	−0.0184 (8)	4.2 (3)
C22a	0.9887 (8)	0.2880 (6)	0.5004 (9)	5.7 (4)	C3c	0.4059 (7)	0.2618 (5)	−0.081 (1)	5.0 (4)
C23a	0.9320 (8)	0.2880 (8)	0.555 (1)	7.7 (5)	C4c	0.3556 (7)	0.1931 (6)	−0.1359 (9)	4.8 (3)
C24a	0.9551 (9)	0.3435 (8)	0.643 (1)	8.3 (5)	C5c	0.4056 (7)	0.1461 (6)	−0.1351 (9)	4.8 (4)
C25a	1.0385 (9)	0.3967 (8)	0.670 (1)	7.7 (5)	C6c	0.5033 (7)	0.1634 (6)	−0.0751 (8)	4.4 (3)
C26a	1.0960 (8)	0.3967 (7)	0.6155 (9)	5.8 (4)	C21c	0.5460 (7)	0.3560 (6)	0.0330 (8)	4.5 (3)
C27a	0.893 (1)	0.345 (1)	0.707 (1)	12.6 (7)	C22c	0.6214 (8)	0.3946 (6)	0.0195 (9)	5.4 (4)
C41a	1.4048 (7)	0.3819 (7)	0.5743 (9)	5.6 (4)	C23c	0.6557 (9)	0.4667 (6)	0.062 (1)	6.2 (4)
C42a	1.4331 (9)	0.3443 (8)	0.644 (1)	7.3 (5)	C24c	0.6133 (8)	0.5012 (6)	0.1162 (9)	5.9 (4)
C43a	1.528 (1)	0.3594 (9)	0.708 (1)	10.0 (6)	C25c	0.5388 (8)	0.4613 (6)	0.129 (1)	6.0 (4)
C44a	1.5933 (9)	0.4168 (9)	0.706 (1)	8.9 (5)	C26c	0.5048 (8)	0.3895 (6)	0.0897 (9)	5.3 (4)
C45a	1.562 (1)	0.4563 (8)	0.641 (1)	9.5 (6)	C27c	0.650 (1)	0.5800 (6)	0.154 (1)	7.6 (5)
C46a	1.4706 (8)	0.4384 (8)	0.577 (1)	8.1 (5)	C41c	0.2535 (7)	0.1733 (6)	−0.1996 (9)	4.8 (3)
C47a	1.701 (1)	0.436 (1)	0.783 (1)	13.4 (8)	C42c	0.2163 (8)	0.2139 (6)	−0.259 (1)	6.5 (4)
C61a	1.1684 (7)	0.3380 (6)	0.2186 (8)	4.5 (3)	C43c	0.1201 (9)	0.1944 (7)	−0.322 (1)	7.0 (5)
C62a	1.1214 (8)	0.3764 (6)	0.1618 (9)	5.4 (4)	C44c	0.0581 (8)	0.1346 (7)	−0.321 (1)	6.7 (4)
C63a	1.1132 (9)	0.3719 (7)	0.0607 (9)	6.7 (4)	C45c	0.0954 (8)	0.0949 (6)	−0.260 (1)	6.0 (4)
C64a	1.1487 (8)	0.3322 (7)	0.007 (1)	7.1 (5)	C46c	0.1931 (8)	0.1142 (6)	−0.198 (1)	5.7 (4)
C65a	1.1991 (9)	0.2939 (7)	0.0673 (9)	6.9 (4)	C47c	−0.0464 (8)	0.1115 (8)	−0.389 (1)	8.5 (5)
C66a	1.2071 (8)	0.2955 (7)	0.1684 (9)	5.8 (4)	C61c	0.5451 (7)	0.1060 (5)	−0.0784 (9)	4.7 (3)
C67a	1.135 (1)	0.327 (1)	−0.105 (1)	11.3 (7)	C62c	0.5891 (7)	0.0871 (5)	0.0075 (9)	4.7 (3)
O1b	0.8046 (4)	0.2545 (3)	0.3056 (5)	3.9 (2)	C63c	0.6190 (8)	0.0302 (6)	0.003 (1)	6.0 (4)
O2b	0.8002 (4)	0.1763 (3)	0.1704 (5)	4.2 (2)	C64c	0.6065 (8)	−0.0135 (6)	−0.089 (1)	6.5 (4)
C12	0.7928 (7)	0.1944 (5)	0.2588 (8)	4.1 (3)	C65c	0.5601 (9)	0.0057 (7)	−0.181 (1)	7.1 (5)
C1b	0.7697 (7)	0.1389 (5)	0.3064 (8)	3.7 (3)	C66c	0.5287 (8)	0.0646 (6)	−0.176 (1)	5.8 (4)
C2b	0.7043 (7)	0.1366 (5)	0.3519 (8)	4.0 (3)	C67c	0.6414 (9)	−0.0761 (6)	−0.096 (1)	8.6 (5)
C3b	0.6836 (8)	0.0844 (6)	0.3983 (9)	4.9 (4)	O	0.703 (2)	0.253 (2)	0.206 (3)	13 (1)*
C4b	0.7275 (8)	0.0340 (6)	0.4032 (9)	4.6 (3)					
				(2) **4**$(Py)_2$					
Rh1	0.000	0.000	0.067	2.99 (2)	C43	0.5897 (9)	0.153 (1)	0.056 (1)	7.4 (5)
Rh2	0.000	0.000	−0.0675 (1)	3.04 (2)	C44	0.6055 (8)	0.2194 (8)	0.0191 (8)	4.7 (4)
O1	0.1085 (4)	0.0435 (4)	0.0663 (5)	3.3 (1)	C45	0.5447 (8)	0.2564 (8)	−0.0154 (9)	5.1 (4)
O2	0.1174 (5)	0.0148 (5)	−0.0576 (5)	3.6 (2)	C46	0.4721 (8)	0.2242 (8)	−0.0184 (8)	4.8 (4)
C11	0.1442 (6)	0.0380 (6)	0.007 (1)	3.5 (2)	C47	0.6842 (9)	0.253 (1)	0.018 (1)	7.2 (5)
C1	0.2262 (6)	0.0622 (6)	0.005 (1)	3.6 (2)	C61	0.2148 (8)	0.1326 (9)	−0.1245 (8)	4.4 (3)
C2	0.2744 (7)	0.0433 (7)	0.0649 (9)	3.9 (2)	C62	0.150 (1)	0.175 (1)	−0.1166 (9)	5.5 (4)
C3	0.3490 (7)	0.0722 (8)	0.067 (1)	4.5 (3)	C63	0.110 (1)	0.206 (1)	−0.182 (1)	8.1 (5)
C4	0.3797 (6)	0.1178 (7)	0.010 (1)	4.3 (3)	C64	0.139 (1)	0.194 (2)	−0.253 (1)	9.3 (7)
C5	0.3326 (7)	0.1332 (7)	−0.0517 (8)	4.0 (3)	C65	0.205 (1)	0.149 (1)	−0.261 (1)	7.8 (6)
C6	0.2563 (6)	0.1069 (7)	−0.0560 (7)	3.4 (2)	C66	0.242 (1)	0.118 (1)	−0.198 (1)	6.9 (5)
C21	0.2498 (8)	−0.0091 (8)	0.1282 (8)	4.1 (3)	C67	0.094 (2)	0.222 (2)	−0.324 (2)	13 (1)
C22	0.2153 (8)	−0.0798 (8)	0.1108 (9)	4.3 (3)	N10	0.000	0.000	0.196 (2)	11 (1)*
C23	0.1951 (9)	−0.1294 (8)	0.168 (1)	5.0 (3)	C101	0.048 (4)	0.018 (8)	0.238 (4)	16 (4)*
C24	0.210 (1)	−0.112 (1)	0.2452 (9)	5.4 (4)	C102	0.061 (5)	0.023 (9)	0.315 (6)	16 (4)*
C25	0.247 (1)	−0.041 (1)	0.258 (1)	6.6 (5)	C103	0.000	0.000	0.364 (6)	18 (4)*
C26	0.2656 (9)	0.0074 (9)	0.201 (1)	5.2 (3)	N20	0.000	0.000	−0.192 (2)	11 (1)*
C27	0.185 (1)	−0.169 (1)	0.305 (1)	8.8 (5)	C201	0.047 (5)	−0.034 (6)	−0.231 (5)	14 (4)*
C41	0.4561 (7)	0.1532 (8)	0.0153 (9)	4.6 (3)	C202	0.053 (5)	−0.039 (6)	−0.313 (8)	13 (4)*
C42	0.5175 (9)	0.119 (1)	0.055 (1)	7.4 (4)	C203	0.000	0.000	−0.350 (6)	12 (4)*

[a] Starred values indicate atoms were refined isotropically. Values for anisotropically refined atoms are given in the form of the isotropic equivalent thermal parameter defined as $(4/3)[a^2\beta_{11} + b^2\beta_{22} + c^2\beta_{33} + ab(\cos\gamma)\beta_{12} + ac(\cos\beta)\beta_{13} + bc(\cos\alpha)\beta_{23}]$.

Table V. Selected Distances (Å) and Bond Angles (deg)[a]

(1) $3(py)_2$

(a) Distances

Rh1–Rh2	2.401 (1)	Rh1–OAc1	2.035 (9)	Rh1–N10	2.20 (2)
Rh1–O1a	2.036 (7)	Rh1–O1b	2.037 (8)	Rh1–O1c	2.049 (6)
Rh2–OAc2	2.041 (8)	Rh2–N20	2.18 (2)	Rh2–O2a	2.052 (7)
Rh2–O2b	2.038 (8)	Rh2–O2c	2.040 (7)	OAc1–C1	1.26 (2)
OAc2–C1	1.28 (1)	C1–C2	1.58 (2)	N10–C101	1.31 (2)
N10–C105	1.32 (1)	C101–C102)	1.37 (2)	C102–C103	1.37 (2)
C103–C104	1.35 (2)	C104–C105	1.40 (2)	N20–C201	1.32 (2)
N20–C205	1.31 (1)	C201–C202	1.39 (2)	C202–C203	1.38 (2)
C203–C204	1.37 (2)	C204–C205	1.41 (2)	OAc1···OAc2	2.27 (1)
O1a···O2a	2.26 (2)	O1b···O2b	2.26 (2)	O1c···O2c	2.25 (2)

(b) Bond Angles

Rh2–Rh1–OAc1	88.3 (2)	Rh2–Rh1–N10	178.7 (3)	Rh2–Rh1–O1a	88.0 (2)
Rh2–Rh1–O1b	88.3 (2)	Rh2–Rh1–O1c	86.0 (2)	OAc1–Rh1–N10	93.1 (4)
OAc1–Rh1–O1a	88.9 (3)	OAc1–Rh1–O1b	176.4 (3)	OAc1–Rh1–O1c	92.1 (3)
N10–Rh1–O1a	92.2 (4)	N10–Rh1–O1b	90.4 (3)	N10–Rh1–O1c	93.8 (4)
O1a–Rh1–O1b	90.1 (3)	O1a–Rh1–O1c	174.0 (3)	O1b–Rh1–O1c	88.6 (3)
Rh1–Rh2–OAc2	87.8 (2)	Rh1–Rh2–N20	179.0 (2)	Rh1–Rh2–O2a	87.2 (2)
Rh1–Rh2–O2b	87.0 (2)	Rh1–Rh2–O2c	88.7 (2)	OAc2–Rh2–N20	91.7 (4)
OAc2–Rh2–O2a	92.2 (3)	OAc2–Rh2–O2b	174.5 (3)	OAc2–Rh2–O2c	89.7 (3)
N20–Rh2–O2a	91.9 (3)	N20–Rh2–O2b	93.6 (4)	N20–Rh2–O2c	92.2 (3)
O2a–Rh2–O2b	89.4 (3)	O2a–Rh2–O2c	175.4 (3)	O2b–Rh2–O2c	88.5 (3)

(2) $4(py)_2$

(a) Distances

Rh1–Rh2	2.374 (3)	C4–C5	1.39 (2)	C42–C43	1.39 (2)
Rh1–O1	2.034 (7)	C4–C41	1.47 (2)	C43–C44	1.37 (2)
Rh1–N10	2.28 (4)	C5–C6	1.41 (2)	C44–C45	1.38 (2)
Rh2–O2	2.066 (8)	C6–C61	1.48 (2)	C44–C47	1.49 (3)
Rh2–N20	2.21 (3)	C21–C22	1.40 (2)	C45–C46	1.38 (2)
O1–C11	1.22 (2)	C21–C26	1.34 (2)	C61–C62	1.36 (2)
O2–C11	1.29 (2)	C22–C23	1.37 (2)	C61–C66	1.40 (2)
C11–C1	1.49 (1)	C23–C24	1.42 (2)	C62–C63	1.45 (3)
C1–C2	1.39 (2)	C24–C25	1.41 (3)	C63–C64	1.37 (3)
C1–C6	1.43 (2)	C24–C27	1.52 (3)	C64–C65	1.40 (3)
C2–C3	1.39 (2)	C25–C26	1.36 (3)	C64–C67	1.56 (4)
C2–C21	1.50 (2)	C41–C42	1.41 (2)	C65–C66	1.40 (3)
C3–C4	1.39 (2)	C41–C46	1.40 (2)	O1···O2	2.25 (2)

(b) Bond Angles

Rh2–Rh1–O1	89.6 (2)	O1–Rh1–N10	90.4 (2)	O1–Rh1–O1	179.2 (3)
O1–Rh1–O1	90.0 (3)	Rh1–Rh2–O2	85.1 (2)	O2–Rh2–N20	94.9 (2)
O2–Rh2–O2	170.3 (4)	O2–Rh2–O2	89.6 (3)		

[a] Numbers in parentheses are estimated standard deviations in the least significant digits.

Table VII. Selected Dihedral Angles (deg) between Mean Planes in the Benzoate Ligands

	$3(py)_2$[a]			
	a	b	c	$4(py)_2$
A–B[b]	51.7	59.6	51.3	47.0
A–C	54.3	18.0	44.6	29.6
A–D	51.1	80.8	55.4	57.7
A–E	50.3	43.7	44.2	41.6

[a] The letters a, b, and c refer to the benzoate ligands in $3(py)_2$. [b] Least-squares planes in the benzoate ligands are noted as follows: A corresponds to the central phenyl ring C1, B to phenyl ring C21, C to phenyl ring C41, and D to phenyl ring C61, and E is the C–CO_2 plane.

Table VIII. Absorption Maxima of **3**, **4**, **5** and the Corresponding Mono- and Bis(pyridine) Adducts[a]

dirhodium carboxylates	solvents	λ_{max}, nm: starting materials	mono-(pyridine) adduct	bis-(pyridine) adduct
3	DCE	640	560	532
	DCE–THF (80:20)	600	554	530
4	DCE	640	572	540
	DCE–THF (80:20)	594	562	538
5	DCE	660	560	520
	DCE–THF (80:20)	608	554	512

[a] λ_{max} ± 1 nm; the calculation gave the corresponding extinction coefficient values within ±1% error.

Table IX. Thermodynamic Constants for the Formation of Mono- and Bis(pyridine) Adducts from **3**, **4**, and **5** (T = 25.0 ± 0.1 °C)

dirhodium carboxylates	K, mol^{-1} L: in DCE	in DCE–THF (80:20)
3	$K_1 = (9 \pm 4) \times 10^8$	$K_1 = (1.1 \pm 0.4) \times 10^7$
	$K_2 = (9 \pm 6) \times 10^4$	$K_2 = (7 \pm 4) \times 10^4$
4	$K_1 = (1.5 \pm 0.5) \times 10^7$	$K_1 = (8 \pm 4) \times 10^6$
	$K_2 = (2 \pm 1) \times 10^4$	$K_2 = (2 \pm 1) \times 10^4$
5	$K_1 = (1.4 \pm 0.4) \times 10^6$	$K_1 = (4 \pm 1) \times 10^4$
	$K_2 = (1.2 \pm 0.4) \times 10^3$	$K_2 = (4 \pm 1) \times 10^2$

and from 6.4 to 8.5 Å along the diagonal. The boxes widen to a larger extent, thus leaving more space for an incoming ligand, in addition to the open window.

An estimate of the height of the boxes in $4(py)_2$ is deduced from the distances of the methyl carbons C27 or C67 to the corresponding O_4 planes. The values obtained are 4.2 and 4.7 Å. The mean value for $3(py)_2$, 4.1 Å, is a little shorter, due to the widening of the boxes. To these distances one should add the contribution from the methyl hydrogens, ca. 2 Å, if one takes into account a 1.2 Å van der Waals radius for H.

The width of a pyridine (between ortho hydrogen atoms) is 4.3 Å[25,26] to which one should add 2.4 Å to account for the van der Waals radius, thus 6.7 Å. The total length, N···para H + 1.2 Å,

(25) Wheeler, W. D.; Poshusta, R. D. *Inorg. Chem.* **1985**, *24*, 3100.
(26) Case, D. A.; Cook, M.; Karplus, M. J. *J. Chem. Phys.* **1980**, *73*, 3294.

Table X. Experimental Formation Rate Constants (k_1, k_2) and Calculated Dissociation Rate Constants ($k_{-1} = k_1/K_1$; $k_{-2} = k_2/K_2$) of Mono- and Bis(pyridine) Adducts

dirhodium carboxylates	solvents	k_1, mol^{-1} L s^{-1}	k_{-1}, s^{-1}	k_2, mol^{-1} L s^{-1}	k_{-2}, s^{-1}
3	DCE	$(5 \pm 2) \times 10^4$	$(5 \pm 4) \times 10^{-5}$	$(1.7 \pm 0.5) \times 10^5$	2.0 ± 1.5
	DCE–THF (80:20)	$(7 \pm 1) \times 10^4$	$(6 \pm 3) \times 10^{-3}$	$(1.5 \pm 0.5) \times 10^5$	2.0 ± 1.5
4	DCE	$(4 \pm 2) \times 10^3$	$(3 \pm 2) \times 10^{-4}$	$(1.5 \pm 0.5) \times 10^5$	7 ± 6
	DCE–THF (80:20)	$(9 \pm 1) \times 10^3$	$(1 \pm 1) \times 10^{-3}$	$(2.0 \pm 1.5) \times 10^5$	10 ± 9
5	DCE	$(1.5 \pm 0.5) \times 10^7$	$(1 \pm 1) \times 10^1$	$>5 \times 10^7$	
	DCE–THF (80:20)	$(2 \pm 1) \times 10^7$	$(6 \pm 4) \times 10^2$	$>5 \times 10^7$	

is 5.1 Å.[25,26] A comparison of these data with the dimensions of the boxes in **4** shows that the pyridine ligands fit tightly but must adopt a diagonal orientation. The ligands are deeply buried in the box in compound **4**(py)$_2$: the total length (7.3 Å = 5.1 Å + 2.2 Å as an average Rh–N bond distance) is close to the depth, with only the para H projecting a little above the edges of the box. These conclusions are also valid qualitatively in the **3** series, the widening of the boxes and the opening of the window obviously relieving some strain around the pyridine ligand. This is illustrated in Figure 6a,b.

Spectrophotometric and Thermodynamic Studies. As can be seen in Figure 1, as the molar ratio pyridine:rhodium carboxylates increases, an isosbestic behavior of the substrates and the 1:1 adducts was observed. This was followed by isosbestic behavior between the 1:1 and the 2:1 adducts. In the course of the adducts formation, all visible absorption bands, in both solvents, shifted to shorter wavelengths (Table VIII).[27–29]

The λ_{max} determined in DCE for the pyridine adducts compare well with the literature data for Rh$_2$(butyrate)$_4$ in dichloromethane.[28] Only for **3** and **4** compared to **5** do shifts of 8–20 nm toward shorter wavelengths occur. In 20% THF, the starting λ_{max} values drop to ca. 600 nm, as expected from the presence at both metallic sites of a better donor than water, in agreement with the analogous effect of another oxygenated ligand (4-picoline *N*-oxide, 595 nm).[28] However the λ_{max} values for the 1:1 and 2:1 adducts are almost identical in both solvents. The differences are less than 10 nm (calculated electronic spectra in Table VIII). These data suggest the formation of a 1:1 adduct whose nature is quite independent of the solvent. The remaining oxygen ligand (water or THF) may be loosely bound, if not lost, after the coordination of the first pyridine molecule.

The equilibrium constants, as determined from a best fit of the absorbance data (Table IX), indicate a greatly reduced coordination of the second pyridine molecule relative to the first one. The observed ratio K_1/K_2 is much greater than that expected statistically for two noninteracting metal centers ($K_1/K_2 = 4$). This ratio, which varies from 10^2 to 10^4 for all the studied species in both solvents, indicates that the effect of pyridine coordination is transmitted through the Rh–Rh bond and is in good agreement with the thermodynamic behavior of other dirhodium(II) tetracarboxylates in the presence of a variety of donor ligands.[29] Comparison of **5** to the hindered carboxylates **3** and **4** shows an increase of the stability of the 1:1 adducts by 2–3 orders of magnitude. A similar effect is observed for the 2:1 adducts but to a smaller extent (1–2 orders of magnitude in K_2 variations). Even if some electronic effects can interfere, most of the large thermodynamic stabilization can clearly be attributed to the rigid walls built around the coordination centers of **3** and **4**.

In contrast to the above results, the solvent effects on the coordination of pyridine to **3**, **4**, and **5** show a similar behavior. The first equilibrium is significantly sensitive to the solvent, K_1 values being lower in THF by factors of ca. 35 for **3** and 80 for **4**, but only a factor of 2 for **5**.

However, the K_2 values of the 2:1 adducts are insensitive to the medium, within the experimental errors, for **3** and **4**, and only slightly sensitive to the medium (by a factor of 3) for **5**. The decrease of K_1 values in the presence of THF can be explained by the competition between the entering pyridine and a better donor ligand than water. The independence of K_2 values from the medium is suggesting again that water or THF dissociates from **3** or **4** during or after the first pyridine association.

These thermodynamic results, although they indicate an effect of the geometry of the hindered carboxylates, are not quite satisfactory (i.e. stability decrease from **3** to **4**) and some "hidden truth" obviously has to be looked for, justifying the following kinetic study.

Kinetic Study. The formation of the 1:1 and 2:1 pyridine adducts of dirhodium carboxylates **3**, **4**, and **5** in DCE and DCE–THF (80:20 by volume) was studied by using a stopped-flow technique at appropriate detection wavelengths (see Experimental Section and Table IX). The corresponding global reactions can be written as follows (A denotes any dirhodium substrate):

$$A + py \underset{k_{-1}}{\overset{k_1}{\rightleftharpoons}} A(py) \quad (1)$$

$$A(py) + py \underset{k_{-2}}{\overset{k_2}{\rightleftharpoons}} A(py)_2 \quad (2)$$

The kinetic parameters k_{-1} and k_{-2} for the corresponding reverse reactions were calculated from the thermodynamic data presented in Table IX. The starting material A(py) for reaction 2 was easily produced at satisfactory concentrations (>92% for **3** and **4**) by mixing equal concentrations of A and py (10^{-4} mol L^{-1}). The values of the experimental formation rate constants and the calculated dissociation rate constants are gathered in Table X.

The slowing down of the rate coordination of one pyridine to the first rhodium center (3–4 orders of magnitude from **5** to **3** and **4**; $k_1(5) \gg k_1(3) > k_1(4)$ reveals the dramatic effect of the large tritolylbenzoate bridges. Bear et al.[30] compared propionate and acetate side chains in dirhodium(II) carboxylates and concluded that the more lipophilic chains push out the axially bound solvent molecules and lead to faster formation rates of the monoadduct. In our case, the k_1 values evaluate the stabilization of the leaving solvent molecule (H_2O and THF) by the walls built around the rhodium sites (Figure 6), if we only consider a dissociative substitution process. It is reasonable to take also in account the steric hindrance encountered by the incoming pyridine in the activated complex. Both features could result in the slower rates for formation of the monopyridine adducts of **3** and **4**. Furthermore, we must note that the k_1 value determined in DCE for the much less hindered dirhodium(II) pivalate (**5**), is in good agreement with the data (10^5–10^7 mol^{-1} L s^{-1}) reported in the literature[31,32] for dirhodium tetraacetate complexes in water. These values correspond to the substitution of a water molecule. However, no significant difference was observed for the substitution of a water molecule or a THF molecule by pyridine within our experimental errors for **3**, **4**, or **5**.

The dissociation of the pyridine molecule from the 1:1 adduct is slowed down to even a larger extent (up to 6 orders of magnitude) than the corresponding formation rates from **5** to **4**. The most inert 1:1 adduct is observed with **3** in DCE. In DCE–THF the bound pyridine is labilized by 1 or 2 orders of magnitude. This

(27) Drago, R. S.; Tanner, P. S.; Richman, R. M.; Long, J. R. *J. Am. Chem. Soc.* **1979**, *101*, 2897.
(28) Drago, R. S.; Long, J. R.; Cosmano, R. *Inorg. Chem.* **1981**, *20*, 2920.
(29) Boyar, E. B.; Robinson, S. D. *Coord. Chem. Rev.* **1983**, *50*, 109 and references therein.
(30) Bear, J. L.; Howard, R. A.; Korn, J. E. *Inorg. Chim. Acta* **1979**, *32*, 123.
(31) Das, K.; Simmons, E. L.; Bear, J. L. *Inorg. Chem.* **1977**, *16*, 1268.
(32) Aquino, M. A. S.; Macartney, D. H. *Inorg. Chem.* **1987**, *26*, 2696.

reveals the participation of the solvent, through the Rh–Rh unit, the largest effect being due the best donor (THF > water).

The binding of the second pyridine molecule occurs 10–100 times faster than that of the first to the same dirhodium species under the same solvent conditions. This behavior was already observed by Das et al.[31] who performed *T*-jump experiments in order to study the binding of pyridine and imidazoles to dirhodium(II) carboxylates. They estimated that the formation of the 2:1 adducts should be much faster (10–100 times) than that of the 1:1 adducts. Using a stopped-flow technique, Aquino et al.[32] have more recently reported that the formation of dirhodium(II) tetraacetate monoadducts with phosphines and phosphites was rate-determining. All these data are suggesting the labilization of the second axial ligand on monoadduct formation, confirming our spectrophotometric and thermodynamic data. This effect seems to be stronger for **4** than for **3**. The values of the rate constants k_2 are quite independent, within experimental errors, of the nature of the leaving solvent molecule and are the same for compounds **3** and **4**.

The dissociation rate constants k_{-2} for the 2:1 adducts are 4–5 orders of magnitude greater than the k_{-1} values for **3** and **4**. It is difficult to estimate the steric effects since it was impossible to obtain kinetic measurements for dirhodium(II) pivalate 2:1 adduct by using a stopped-flow technique. However, the lability of the second pyridine molecule seems to increase from **3** to **4**.

Interpretation of the Catalytic Results. If we go back to the problem of catalytic activity, we can use the above results to imagine the geometry and accessibility of a carbenic fragment attached to one of the rhodium atoms. The shape of a carbethoxycarbene is very different from that of a pyridine, and a width of ca. 5.8–6 Å can be estimated if we assume a planar H—C(carbene)—C=O arrangement. However, as in the case of pyridine, the carbene can only be accommodated in a diagonal orientation with regard to the walls and is deeply buried in the box. If we consider the reactive site of the carbene fragment, viz. the carbon attached to the rhodium, it must be hidden and totally inaccessible in the case of **4** and only accessible from the narrow "window" side of **3**.

As a consequence, it is clear that, in **4** (and this is valid for any compound of the **2** series), no reaction of such a carbene, even with a terminal olefin, would be expected, and this is observed experimentally. One may even ask whether the formation of an intermediate carbene is conceivable: in the initial step of the catalytic cycle the reagent will coordinate to the metal and the increase in size on going from a trigonal diazo ester to a tetrahedral coordinated diazonium (prior to the loss of N_2) may be prohibitive. However, the rapid transformation of the products of the **2** series and the concomitant absence of N_2 evolution, in the presence of a diazo ester, plead for the occurrence of some reaction with one or a very limited number of equivalents of the diazo ester followed, in the absence of coupling with an olefin, by an irreversible decomposition (spectra run on the resulting solution showed the absence of any UV/visible absorption characteristic for dimeric rhodium(II) compounds).

If we repeat the operation, viz. replacing a pyridine by a carbene ligand, but with complex **3**, the result is very different. The carbene does not "scratch" the walls any more, the large ethoxycarbonyl fragment being presumably directed toward the acetate ("window" side). At this stage, the olefin is still able to approach and react with the carbene. However, the fact that the reaction has to be run at temperature >50 °C to achieve an acceptable rate shows that the steric hindrance still plays a major role (similar rates are observed with unhindered catalysts at ca 10–20 °C). This is in agreement with the large differences observed for the pyridine coordination between rhodium(II) pivalate and **3**.

The stereoselectivity of the cyclopropanation was discussed by Doyle[1,5] and the preference for *anti*-cyclopropane formation from diazo esters interpreted in terms of an interaction between the oxygen doublets and a developing charge on an olefinic carbon. Although this effect may play some role in our case, as perhaps examplified by the rather low (2–4) syn selectivity, it is clear that steric considerations are of major importance.

One should consider two factors: the geometry of the carbene and the way the olefin approaches the reactive center. It is quite clear that the cyclohexene can only be accommodated if the saturated carbons are left behind in the window, their insertion between the carbene and the walls being highly improbable. There remain two possibilities: the carboxylate group may point inside the cavity (toward the walls) or outside (toward the window), the resulting cyclopropanes having anti and syn geometries, respectively. The syn selectivity observed by using the dirhodium(II) tris(triarylbenzoate) series reflects the preference for the carbenecarboxylate to point toward the open side (window side) of the catalytic site.

Supplementary Material Available: Listings of anisotropic thermal parameters (Table IIIS), complete bond distances and angles (Table IVS), and least-squares planes (Table VIS) for $3(py)_2$ and $4(py)_2$, a numbering scheme for the two compounds, and figures showing titration curves and calculated electronic spectra for **3–5** (15 pages); listings of observed and calculated structure factors for $3(py)_2$ and $4(py)_2$ (37 pages). Ordering information is given on any current masthead page.